CHEMISTRY OF MATERIALS

VOLUME 21, NUMBER 6 MARCH 24, 2009

Communications

Tetragonally Perforated Layer Structure via Columnar Ordering of 4′-(3,4,5-Trioctyloxybenzoyloxy)benzoic Acid in a Supramolecular Complex with Polystyrene-*block*-Poly(4-vinylpyridine)

Wei-Tsung Chuang,[†] Hwo-Shuenn Sheu,*[,†] U-Ser Jeng,*[,†] Hou-Hsi Wu,[‡] Po-Da Hong,[‡] and Jey-Jau Lee[†]

National Synchrotron Radiation Research Center, Hsinchu 300, Taiwan, and Department of Polymer Engineering, National Taiwan University of Science and Technology, Taipei 106, Taiwan

Received December 22, 2008
Revised Manuscript Received February 9, 2009

During the past decade, supramolecular side-chain liquid-crystalline block copolymers have attracted considerable attention due to their capability in self-assembling into the so-called *structure-within-structure*, which is characterized by a locally ordered liquid-crystalline (LC) phase, of an ordering length scale of 1−10 nm, intercalated into the microphase-separated and ordered block copolymers of lattice parameters of 10−100 nm.[1−4] Such a type of hierarchical assembly greatly stimulates applications in multifunctional materials.[1,2] The pioneer group of Ikkala[2] showed that pentadecylphenol (PDP) surfactants could passively form a smectic phase in the microdomains of poly(styrene)-*block*-poly(4-vinylpyridine) (PS-*b*-P4VP), whose microphase separation was still dominated by the two repulsive dissimilar copolymer blocks. Recently, monodendritic or wedge-shaped side-groups nonconvalently attached to homopolymers were shown to actively self-assembly into locally ordered columnar LC structures;[5,6] however, there was no report in using such columnar LC phase to form hierarchical microphase separation in diblock copolymers.

Scheme 1. Cartoon for the Supramolecular Assembly Routes of the Diblock Copolymer PS-*b*-P4VP(TOB)$_x$

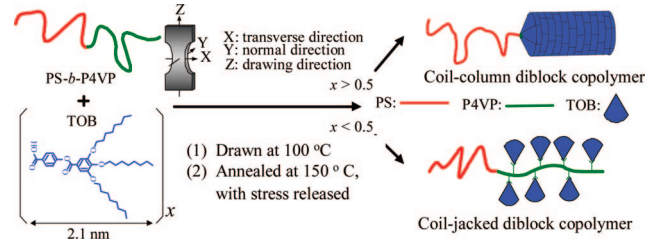

In this study, we have grafted a specially designed nonmesogenic 4′-(3,4,5-trioctyloxybenzoyloxy)benzoic acid (TOB) to the P4VP block (Scheme 1) of a symmetric PS_{192}-*b*-$P4VP_{181}$ to form LC side chains in the supramolecular complex. Compared to the amphiphilic molecules of a linear

* Corresponding authors. E-mail: hsheu@nsrrc.org.tw; usjeng@nsrrc.org.tw.
[†] National Synchrotron Radiation Research Center.
[‡] National Taiwan University of Science and Technology.

(1) *Supramolecular polymer*; Ciferi, A., Ed.; Taylor & Francis: Boca Raton, 2005.
(2) (a) Ruokolainen, J.; Mäkinen, R.; Torkkei, M.; Mäkelä, T.; Serimaa, R.; ten Brinke, G.; Ikkala, O. *Science* **1998**, *280*, 557–560. (b) Ikkala, O.; ten Brinke, G. *Science* **2002**, *295*, 2407–2409. (c) Valkama, S.; Ruotsalainen, T.; Nykänen, A.; Laiho, A.; Kosonen, H.; ten Brinke, G.; Ikkala, O.; Ruokolainen, J. *Macromolecules* **2006**, *39*, 9327–9336.
(3) Chen, H.-L.; Lu, J.-S.; Yu, C.-H.; Yeh, C.-L.; Jeng, U. -S.; Chen, W.-C. *Macromolecules* **2007**, *40*, 3271–3276.
(4) Tenneti, K. K.; Chen, X.; Li, C. Y.; Wan, X.; Fan, X.; Zhou, Q. F.; Rong, L.; Hsiao, B. S. *Macromolecules* **2007**, *40*, 5095–5102.
(5) Percec, V.; Glodde, M.; Bera, T. K.; Miura, Y.; Shiyanovskaya, I.; Singer, K. D.; Balagurusamy, V. S. K.; Heniney, P. A.; Schenll, I.; Rapp, A.; Spiess, H.-W.; Huason, S. D.; Duan, H. *Nature* **2002**, *419*, 384–387.
(6) (a) Beginn, U. *Prog. Polym. Sci.* **2003**, *28*, 1049–1105. (b) Zhu, X.; Beginn, U.; Möller, M.; Gearba, R. I.; Anokhin, D. V.; Ivanov, D. I. *J. Am. Chem. Soc.* **2006**, *128*, 16928–16937.

10.1021/cm803449g CCC: $40.75
Published on Web 02/25/2009

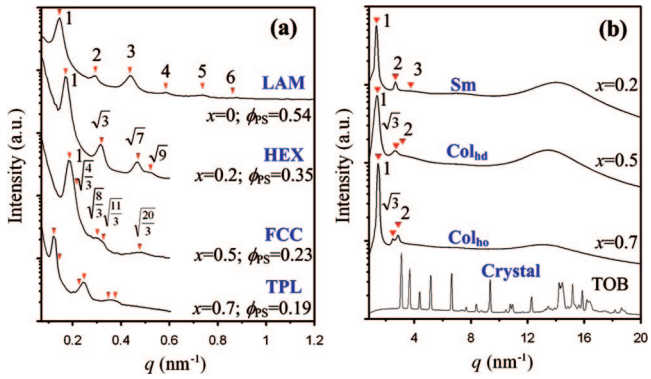

Figure 1. SAXS (a) and WAXS (b) profiles of PS-*b*-P4VP(TOB)$_x$. The scattering peaks are indexed based on LAM, HEX, FCC, and TPL in SAXS and Sm, Col$_{hd}$, and Col$_{ho}$ in WAXS, respectively. Also shown is the WAXS profile of pure TOB for comparison; all the WAXS profiles of PS-*b*-P4VP(TOB)$_x$ indicate no TOB crystalline domains.

shape often used in the comb−coil diblock copolymers,[2,3] the amphiphilic nonmesogen of TOB features in its three alkene tails expanding out for a wedge-like shape and the extended benzoic acid head for both hydrogen bonding with P4VP and $\pi-\pi$ stacking in self-alignment. With these designated characteristics for a prominent self-assembly nature with P4VP, we demonstrate that TOB can induce several LC phases of the supramolecular complex of P4VP(TOB)$_x$ depending on the overall binding fraction ratio x; the highly ordered LC phases drastically influence the global morphology of the system. When blended with PS-*b*-P4VP, TOB would prefer to bind to pyridine of P4VP rather than aggregate, as revealed by the X-ray diffraction result (Figure 1b) and the characteristic FTIR absorptions of the carboxylic acid and pyridine (cf. Figure S4, Supporting Information). Therefore, x is approximated by the prescribed ratio of TOB molecules to 4VP monomers of the copolymers in this study. Solution casting thin films of PS-*b*-P4VP(TOB)$_x$ were subject to thermal annealing at 100 °C under stretching to critically facilitate the microphase separation; after tension was released, the freestanding films were furthermore thermally annealed at 150 °C for highly ordered hierarchical structures. Elucidated by synchrotron-based small and wide-angle X-ray scattering (SAXS and WAXS) and transmission electron microscopy (TEM), the global structure of PS-*b*-P4VP(TOB)$_x$ transforms from lamellar (LAM), hexagonal (HEX), face-centered-cubic (FCC) to tetragonally perforated layer (TPL) structures, as the locally ordered P4VP(TOB)$_x$changes from smectic (Sm) phase, hexagonal phase packed by disordered columns (Col$_{hd}$), to hexagonal phase packed by ordered columns (Col$_{ho}$), upon the increase of TOB content.

Illustrated in Figure 1a,b are a series of SAXS and WAXS profiles for the samples of x values ranging from 0 to 0.7 (equivalent to volume fractions of PS, ϕ_{PS}, from 0.54 to 0.19). For the neat copolymer with $x = 0$, six lamellar peaks in the SAXS profile (Figure 1a) with relatively stronger peak intensities for odd-order reflections indicate that the PS and P4VP microdomains have the same layer thickness $d = 43$ nm, which is extracted from the first scattering peak position at $q = 0.146$ nm^{-1}. Here, the scattering wavevector $q = 4\pi(\sin\theta)/\lambda$ is defined by the scattering angle 2θ and wavelength λ of X-rays. With $x = 0.2$ ($\phi_{PS} = 0.35$), the SAXS profile exhibits a set of scattering peaks with a peak position ratio of $1:3^{1/2}:7^{1/2}:3$ (Figure 1a). The result implies that the PS cylinder domains, following the typical phase behavior of diblock copolymers, are hexagonally packed with a lattice parameter $a = 37$ nm (extracted from the first peak position $q_{(100)} = 0.17$ nm^{-1}). Correspondingly, the WAXS profile (Figure 1b) shows a set of smectic scattering peaks starting with the 1.33 nm^{-1} peak, indicating that the P4VP(TOB)$_{0.2}$ forms a local smectic structure with inter-lamellar distance of 4.7 nm. The SAXS and WAXS results together suggest a *cylinders-within-lamellae* structure for PS-*b*-P4VP(TOB)$_{0.2}$.

With an increased TOB content to $x = 0.5$ ($\phi_{PS} = 0.23$), the SAXS pattern exhibits ordered powder rings arranged in the characteristic peak position ratio of $1:(4/3)^{1/2}:(8/3)^{1/2}:(11/3)^{1/2}:(20/3)^{1/2}$ (Figure 1a) of the FCC structure,[7] with a corresponding lattice parameter $a = 58.5$ nm. Dominated by the microphase separation of the two copolymer blocks, PS with $\phi_{PS} = 0.23$ forms spheres in the FCC structure, as evidenced by the TEM image (Figure S5, Supporting Information). Moreover, the corresponding WAXS pattern exhibits three powder rings with a peak position ratio of $1:3^{1/2}:2$ (Figures 1b), revealing a hexagonal columnar mesophase formed by the supramolecular blocks of P4VP(TOB)$_{0.5}$ with a lattice parameter $a = 4.5$ nm. On the basis of the WAXS result of powder-ring like scattering, these hexagonally packed P4VP(TOB)$_{0.5}$ columnar domains are randomly oriented (Col$_{hd}$), due likely to the columns with unsaturated TOB grafting being not rigid enough. Integrated SAXS and WAXS results suggest that the FCC-packed PS spheres are intercalated in the matrix of disordered columnar phase Col$_{hd}$ of P4VP(TOB)$_{0.5}$.

At a high TOB content of $x = 0.7$, the columns of P4VP(TOB)$_{0.7}$ preferentially orientate in the direction of prestretching (Z), resulting in anisotropic WAXS patterns (near the center areas of Figure 2d,e) that emphasize in the equatorial direction with the signature peaks (peak position ratio $= 1:3^{1/2}:2$) of the Col$_{ho}$. In addition, asymmetrical and broad WAXS humps contributed by TOB indicate that TOB molecules are aligned in an axis approximately 55° titled from the columnar axis (Figures 2e and S6, Supporting Information). The extracted lattice parameter $a = 4.1$ nm of the Col$_{ho}$ phase of P4VP(TOB)$_{0.7}$ is smaller than that (4.5 nm) of the Col$_{hd}$ phase at $x = 0.5$, implying a tighter, namely, more rigid packing of the Col$_{ho}$ structure. Consequently, the corresponding 2-D SAXS images demonstrate single crystal-line-like reflections (Figure 2), especially when the beam is incident with the film normal direction. Characterized by a set of strong lamellae-like reflections in the meridian direction and two weaker satellite sets of similar reflections at off-meridian positions, the SAXS pattern of PS-*b*-P4VP(TOB)$_{0.7}$ in Figure 2a is reminiscent of a perforated

(7) Huang, Y. Y.; Chen, H. L.; Hashimoto, T. *Macromolecules* **2003**, *36*, 764–770.

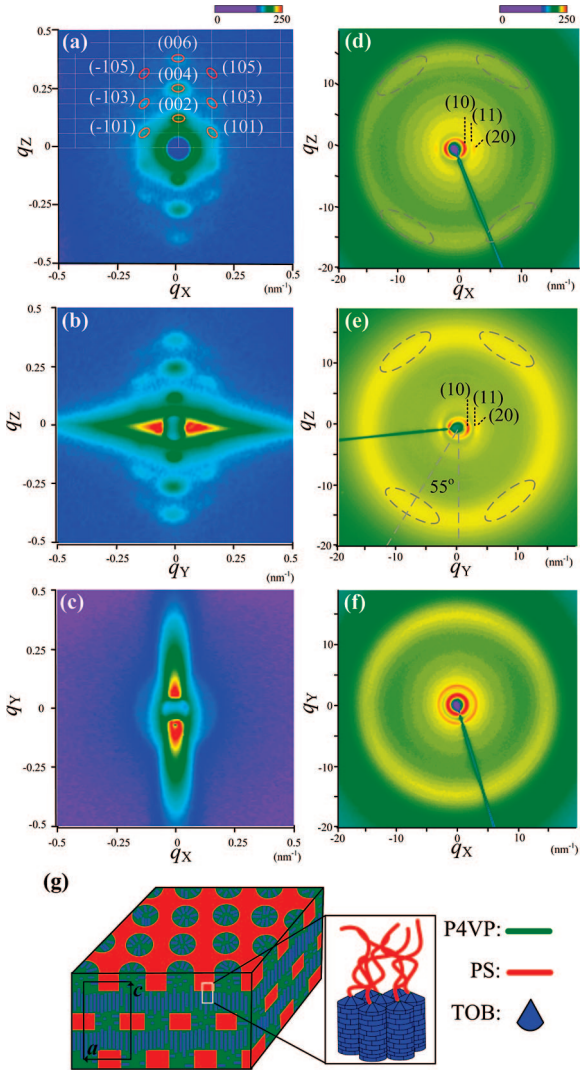

Figure 2. Subsequent 2D SAXS (a−c) and WAXS (d−f) patterns for PS-*b*-P4VP(TOB)$_{0.7}$ with X-ray beam respectively along the *Y*-, *X*-, and *Z*-directions defined in Scheme 1. The reflections are indexed according to the body-centered tetragonal lattice (SAXS) and HEX (WAXS). (g) Cartoon for the *TPL-within-column* structure of PS-*b*-P4VP(TOB)$_{0.7}$.

layer structure.[8] The intensified lamellar reflections favor a layer-based structure more than a BCC or FCC structure. Using a body-centered tetragonal (*I*4/*mmm* space group) lattice of ABAB layers stacking with lattice parameters $a = b = 47.4$ nm and $c = 102.6$ nm for the perforated pore spacing and layer stacking, respectively, we can index all the reflections in Figure 2a. Moreover, with a beam nearly parallel to the film, a similar SAXS pattern can also be obtained (Figure 2b), and this result supports the TPL structure proposed. With an incident beam orthogonal to the previous two directions (i.e., along the long dimension of the sample), however, no clear SAXS pattern can be identified (Figure 2c) likely because of a serious scattering smearing in this direction of a long sample path length for

(8) (a) Hamley, I. W.; Koppi, K. A.; Rosedale, J. H.; Bates, F. S.; Almdal, K.; Mortensen, K. *Macromolecules* **1993**, *26*, 5959–5970. (b) Schulz, M. F.; Khandpur, A. K.; Bates, F. S.; Almdal, K.; Mortensen, K.; Hajduk, D. A.; Gruner, S. M. *Macromolecules* **1996**, *29*, 2857–2867. (c) Zhu, L.; Huang, P.; Cheng, S. Z. D.; Ge, Q.; Quirk, R. P.; Thomas, E. L.; Lotz, B.; Wittmann, J.-C.; Hsiao, B. S.; Yeh, F.; Liu, L. *Phys. Rev. Lett.* **2001**, *86*, 6030–6033.

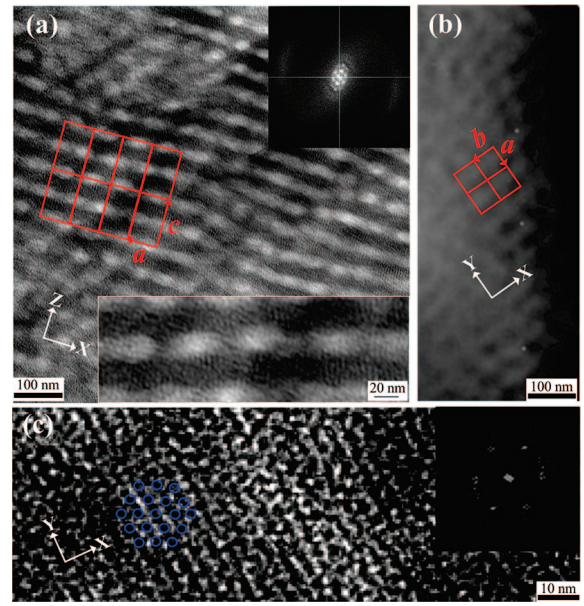

Figure 3. TEM images of the microtomed sections of PS-*b*-P4VP(TOB)$_{0.7}$ (with I_2-stained P4VP domains in black) cut along the *XZ* plane for a side-view of the *TPL-within-columnar* structure in (a), the XY plane for a single PS layer perforated with P4VP(TOB)$_{0.7}$ domains in (b), and another XY plane for a top-view of the hexagonally packed columns of P4VP(TOB)$_{0.7}$ in (c), with the corresponding FFT shown in the inset.

X-rays. Figure 2g illustrates the proposed *TPL-within-columnar* microstructure of PS-*b*-P4VP(TOB)$_{0.7}$, based on the X-ray scattering results. The TPL structure is furthermore confirmed by the TEM images in Figure 3; the formation of LC phase of TOB is evidenced by birefringence patterns with polarized optical microscopy (POM) (cf. Figure S7, Supporting Information).

A TEM image of the microtomed section cut along the PS-*b*-P4VP(TOB)$_{0.7}$ film normal (Figure 3a) displays the side view of the perforation layer of the *TPL-within-column* structure, which consists of PS layers (discontinuous bright zones) perforated with the columnar phase of P4VP(TOB)$_{0.7}$. The zoom-in view of Figure 3a details straight columns (alternated dark and white strips) between PS layers. The tetragonal lattice with ABAB stacking can be clearly identified from the real-space image. The corresponding fast Fourier transform (FFT) of the TEM image in the inset of Figure 3a matches the scattering pattern observed by SAXS in the reciprocal space (cf. Figure 2a), whereas the faint arcs by the sides are also consistent with the WAXS result (cf. Figure 2d) for the ordered columns of the supramolecular complex P4VP(TOB)$_{0.7}$. In general, the columns are oriented normal to PS layers or the intermaterial dividing surface (IMDS) of the PS-*b*-P4VP. TEM image of a microtomed section cut along one single PS layer illustrates the PS layer perforated with the P4VP(TOB)$_{0.7}$ columns for the in-plane tetragonal lattice packing (Figure 3b). Whereas the TEM image for the section cut along one single P4VP layer (Figure 3c) demonstrates a top view of the highly ordered, hexagonally packed columns (Col_{ho}), FFT of the corresponding TEM image (inset of Figure 3c) presents the characteristic six-spot pattern of the hexagonal phase. The average distance between P4VP(TOB)$_{0.7}$ columns extracted from the TEM image is approximately 4 nm, which closely matches that, 4.1 nm, extracted from the SAXS result previously.

Coil−coil diblock copolymers[8] often microphase separate into lattices of high symmetry, such as a hexagonally packed or body-centered-cubic structure. Formation of an anomalous tetragonal lattice with a comb−coil system of cylindrical microdomains was made possible by grafting linear-type surfactants in the supramolecular comb blocks for a special orientation of the mesomorphic lamellar phase (Sm) with respect to the cylinder domains, as demonstrated by Chen et al. recently;[3] the tetragonal lattice, however, was not stable, and the system fell back to the morphology of hexagonally packed cylinders at high surfactant grafting density. Compared to previous supramolecular block copolymer systems with essentially a Sm matrix,[2,3] the present system can form a well-organized and stable TPL structure based the rigid Col_{ho} phase of P4VP(TOB)$_{0.7}$. Presumably, with the three bulky alkene tails and the strong $\pi-\pi$ stacking of the benzoic acid, TOB can form rigid columns with P4VP at a high grafting density, and the system behaves as a rod−coil copolymer.[9] As a result, the supramolecular complex P4VP(TOB)$_{0.7}$ not only packs into layers but also forms the TPL structure (Figure 2g) with PS domains of a nonconstant curvature (Figure 3b). At a slightly lower TOB grafting density of $x = 0.5$, the P4VP(TOB)$_{0.5}$ columns may not be rigid enough, and the PS free energy dominates the microphase separation of the system, leading to FCC-packed spherical PS domains (for minimizing surface energy) within the Col_{hd} phase (Figure 1). Since the PS volume fractions of the two FCC ($\phi_{PS} = 0.23$) and TPL ($\phi_{PS} = 0.19$) systems do not differ much, therefore, the transition from TPL to FCC may be attributed to a reduced packing energy of the softened P4VP(TOB)$_x$ columns at a smaller TOB grafting density (i.e., $x = 0.5$). We note that a slight distortion of FCC spheres resembles a TPL structure.

In summary, simply by adjusting TOB grafting density for a wide range of mesomorphic orderings of P4VP(TOB)$_x$ from Sm, Col_{hd}, to Col_{ho} phases, we have demonstrated that the global morphology of PS-*b*-P4VP(TOB)$_x$ can be tuned from LAM, HEX, FCC, to TPL, successively. As the hydrogen bonding between P4VP and TOB is temperature-sensitive, it is also possible to tune the mesomorphic ordering of P4VP(TOB)$_x$ via its response to temperature and thus change the globally ordered morphology of the system.

Supporting Information Available: Synthesis route and thermal characterizations of TOB, FTIR spectra, POM and TEM micrographs, and X-ray scattering measurement details (PDF). This material is available free of charge via the Internet at http://pubs.acs.org.

CM803449G

(9) Lee, M.; Cho, B.-Y.; Zin, W.-C. *Chem. Rev.* **2001**, *101*, 3869–3892.